

AD-A280 141

NASA Contractor Report 194892



ICASE Report No. 94-17

(1)



ICASE

EVALUATION OF REYNOLDS STRESS TURBULENCE CLOSURES IN COMPRESSIBLE HOMOGENEOUS SHEAR FLOW

DTIC
ELECTE
JUN 01 1994
S F D

C. G. Speziale
R. Abid
N. N. Mansour

312 94-16200



This document has been approved
for public release and sale; its
distribution is unlimited.

DOC QUALITY CHECKED

Contract NAS1-19480
March 1994

Institute for Computer Applications in Science and Engineering
NASA Langley Research Center
Hampton, VA 23681-0001



Operated by Universities Space Research Association

94 5 31 033

ICASE Fluid Mechanics

Due to increasing research being conducted at ICASE in the field of fluid mechanics, future ICASE reports in this area of research will be printed with a green cover. Applied and numerical mathematics reports will have the familiar blue cover, while computer science reports will have yellow covers. In all other aspects the reports will remain the same; in particular, they will continue to be submitted to the appropriate journals or conferences for formal publication.

Accession For		
NTIS	CRA&I	<input checked="" type="checkbox"/>
DTIC	TAB	<input type="checkbox"/>
Unannounced <input type="checkbox"/>		
Justification		
By		
Distribution /		
Availability Codes		
Dist	Avail and / or Special	
A-1		

EVALUATION OF REYNOLDS STRESS TURBULENCE CLOSURES IN COMPRESSIBLE HOMOGENEOUS SHEAR FLOW

C. G. Speziale*

**Aerospace & Mechanical Engineering Department
Boston University
Boston, MA 02215**

R. Abid

**High Technology Corporation
NASA Langley Research Center
Hampton, VA 23681**

N. N. Mansour

**NASA Ames Research Center
Moffett Field, CA 94035**

ABSTRACT

Direct numerical simulation data bases for compressible homogeneous shear flow are used to evaluate the performance of recently proposed Reynolds stress closures for compressible turbulence. Three independent pressure-strain models are considered along with a variety of explicit compressible corrections that account for dilatational dissipation and pressure-dilatation effects. The ability of the models to predict both time evolving fields and equilibrium states is systematically tested. Consistent with earlier studies, it is found that the addition of simple dilatational models allows for the prediction of the reduced growth rate of turbulent kinetic energy in compressible homogeneous shear flow. However, a closer examination of the equilibrium structural parameters uncovers a major problem. None of the models are able to predict the dramatic increase in the normal Reynolds stress anisotropies or the significant decrease in the Reynolds shear stress anisotropy that arise from compressible effects. The physical origin of this deficiency is attributed to the neglect of compressible terms in the modeling of the deviatoric part of the pressure-strain correlation.

*This research was supported by the National Aeronautics and Space Administration under NASA Contract No. NAS1-19480 while the author was in residence at the Institute for Computer Applications in Science and Engineering (ICASE), NASA Langley Research Center, Hampton, VA 23681-0001.

1. INTRODUCTION

The need to predict supersonic and hypersonic turbulent flows of aerodynamic importance has, in recent years, led to new research initiatives in compressible turbulence modeling. A major stumbling block in the development of improved compressible turbulence models is the lack of detailed experimental data for the compressible turbulence statistics in basic high-speed compressible flows. Experimental limitations currently make it infeasible to obtain detailed measurements of any turbulence statistics beyond the mean velocity and Reynolds shear stress in supersonic turbulent flows. This makes it virtually impossible to pinpoint the origin of deficient model predictions when they arise. In Reynolds averaged calculations of complex supersonic turbulent flows, erroneous predictions for the mean velocity field may arise from modeling errors in the Reynolds stresses that can be traced to a variety of possible deficiencies in the treatment of compressibility effects.

During the past four years, direct numerical simulation (DNS) data bases of some basic supersonic turbulent flows have become available [1, 2], wherein the full compressible Navier-Stokes, continuity and energy equations are solved numerically with all turbulent scales resolved. Most notable among these are the DNS data bases for compressible homogeneous shear flow (see Blaisdell, Mansour and Reynolds [3] and Sarkar, Erlebacher and Hussaini [4,5]). Homogeneous shear flow is an important building-block flow since it encapsulates some of the important features of an equilibrium turbulent boundary layer in a simplified setting that is unencumbered by the effects of turbulent diffusion or wall blocking. It has been an extremely useful test case for the calibration and screening of turbulence models for incompressible flows [6-8]. However, no comprehensive test of compressible Reynolds stress models has been made using these new DNS data bases for compressible homogeneous shear flow. This establishes the motivation for the present paper. Prior to this study, only very limited comparisons of compressible turbulence models have been made using these DNS results [9,10].

In this paper, the DNS data base of Blaisdell, Mansour and Reynolds [3] for compressible homogeneous shear flow will be used to critically evaluate recently proposed compressible Reynolds stress closures. Full second-order closures will be considered that explicitly account for high-speed compressible effects. Variable density extensions of three incompressible pressure-strain models due to Launder and co-workers [11, 12] and Speziale, Sarkar and Gatski [13] will be tested along with models for the compressible dissipation and pressure-dilatation that were recently proposed by Sarkar *et al* [14,15] and Zeman [16,17]. The ability of each model to predict time-evolving fields and equilibrium states such as the Reynolds stress anisotropies will be assessed in detail. An attempt will also be made to understand the physical origin of deficient model predictions. In this regard, some important results will

be uncovered that were overlooked in previous studies. These issues will be discussed fully in the sections to follow and a recommendation will be made for the development of improved models.

2. THEORETICAL BACKGROUND

We will consider the mean turbulent flow of an ideal gas governed by the compressible Navier-Stokes equations. The mass density ρ is decomposed into standard ensemble mean and fluctuating parts, respectively, as follows:

$$\rho = \bar{\rho} + \rho'. \quad (2.1)$$

The velocity field u_i and temperature T are decomposed into standard ensemble mean and fluctuating parts given by

$$u_i = \bar{u}_i + u'_i, \quad T = \bar{T} + T' \quad (2.2)$$

or into mass-weighted mean and fluctuating parts given by

$$u_i = \tilde{u}_i + u''_i, \quad T = \tilde{T} + T''. \quad (2.3)$$

For any flow variable \mathcal{F} , the quantity $\tilde{\mathcal{F}} \equiv \overline{\rho\mathcal{F}}/\bar{\rho}$ denotes the Favre or mass-weighted average given that an overbar represents a standard ensemble mean.

The Favre-averaged continuity, Navier-Stokes and energy equations take the form [18, 19]

$$\frac{\partial \bar{\rho}}{\partial t} + (\bar{\rho}\bar{u}_i)_{,i} = 0 \quad (2.4)$$

$$\frac{\partial}{\partial t}(\bar{\rho}\bar{u}_i) + (\bar{\rho}\bar{u}_i\bar{u}_j)_{,j} = -\bar{p}_{,i} \quad (2.5)$$

$$\frac{\partial}{\partial t}(\bar{\rho}\bar{C}_v\bar{T}) + (\bar{\rho}\bar{C}_v\bar{T}\bar{u}_i)_{,i} = -\bar{p}\bar{u}_{i,i} - \overline{p'u'_{i,i}} + \Phi \quad (2.6)$$

in homogeneous turbulent flows where the mean velocity gradients and all higher-order statistics are spatially uniform. In Eqs. (2.5) and (2.6),

$$p = \rho RT \quad (2.7)$$

$$\Phi = \sigma_{ij}u_{i,j} \quad (2.8)$$

$$\sigma_{ij} = -\frac{2}{3}\mu u_{k,k}\delta_{ij} + \mu(u_{i,j} + u_{j,i}) \quad (2.9)$$

are, respectively, the thermodynamic pressure, viscous dissipation and viscous stress tensor; R is the ideal gas constant, C_v is the specific heat at constant volume, μ is the dynamic

viscosity of the gas, and $(\cdot)_{,i} \equiv \partial(\cdot)/\partial x_i$ denotes a spatial gradient. Since the turbulent mass flux $\bar{\rho}\bar{u}_i''$ vanishes in compressible homogeneous turbulence, it follows that [19]

$$\bar{\Phi} = \bar{\sigma}_{ij}\bar{u}_{i,j} + \bar{\rho}\epsilon \approx \bar{\rho}\epsilon \quad (2.10)$$

at high turbulence Reynolds numbers where $\epsilon \equiv \overline{\sigma'_{ij}u'_{i,j}}/\bar{\rho}$ is the turbulent dissipation rate.

Following the recent work of Sarkar *et al* [14] and Zeman [16], the turbulent dissipation rate can be decomposed into solenoidal and dilatational parts as follows:

$$\epsilon = \epsilon_s + \epsilon_c \quad (2.11)$$

where, for homogeneous turbulence,

$$\epsilon_s = \overline{\mu\omega'_i\omega'_i}/\bar{\rho}, \quad \epsilon_c = \frac{4}{3}\overline{\mu(u'_{i,i})^2}/\bar{\rho} \quad (2.12)$$

are, respectively, the solenoidal and compressible (or dilatational) parts of the turbulent dissipation rate given that ω'_i is the fluctuating vorticity. Here, ϵ_s represents the turbulent dissipation arising from the traditional energy cascade which is solenoidal (i.e., vortical) in character; ϵ_c represents the turbulent dissipation arising from purely compressible or dilatational modes ($\epsilon_c = 0$ for incompressible turbulent flows). For homogeneous turbulence, this decomposition is unique.

Since the mean pressure

$$\bar{p} = \bar{\rho}RT, \quad (2.13)$$

it is clear from (2.4)-(2.10) that closure of the mean flow equations is achieved in compressible homogeneous turbulence, at high Reynolds numbers, once models for the pressure-dilatation, compressible dissipation and solenoidal dissipation are provided. The determination of these correlations also requires information on the turbulence intensity level and, hence, on the Reynolds stress tensor. The Favre-averaged Reynolds stress tensor $\tau_{ij} \equiv \bar{u}_i''\bar{u}_j''$ is a solution of the transport equation [18, 19]

$$\bar{\rho}\dot{\tau}_{ij} = -\bar{\rho}\tau_{ik}\bar{u}_{j,k} - \bar{\rho}\tau_{jk}\bar{u}_{i,k} + \Pi_{ij} - \frac{2}{3}\bar{\rho}\epsilon\delta_{ij} + \frac{2}{3}\overline{p'u'_{k,k}}\delta_{ij} \quad (2.14)$$

which is exact for compressible homogeneous turbulence given that

$$\begin{aligned} \Pi_{ij} &= \overline{p'(u'_{i,j} + u'_{j,i})} - \frac{2}{3}\overline{p'u'_{k,k}}\delta_{ij} \\ &\quad - \left(\overline{\sigma'_{ik}u'_{j,k} + \sigma'_{jk}u'_{i,k}} - \frac{2}{3}\overline{\sigma'_{kl}u'_{l,k}}\delta_{ij} \right) \end{aligned} \quad (2.15)$$

is the difference between the deviatoric parts of the pressure-strain correlation and dissipation rate tensor. Eq. (2.14) contains the pressure-dilatation correlation $\overline{p'u'_{k,k}}$ as well as the

compressible and solenoidal parts of the dissipation rate tensor since $\varepsilon = \varepsilon_s + \varepsilon_c$. Hence, a full Reynolds stress closure is achieved in compressible turbulence if models are provided for:

- (i) The difference between the deviatoric parts of the pressure-strain correlation and dissipation rate tensor, Π_{ij} .
- (ii) The pressure-dilatation correlation $\overline{p' u'_{i,i}}$.
- (iii) The solenoidal dissipation ε_s .
- (iv) The compressible dissipation ε_c .

In compressible homogeneous shear flow, the mean velocity gradient tensor is given by

$$\tilde{u}_{i,j} = S\delta_{i1}\delta_{j2} \quad (2.16)$$

where S is the shear rate which is constant. The mean density is constant whereas the mean temperature is a function of time alone, i.e.,

$$\bar{\rho} = \text{constant} \quad (2.17)$$

$$\tilde{T} = \tilde{T}(t). \quad (2.18)$$

Eqs. (2.16) and (2.17), which are the same as their incompressible counterparts, identically satisfy the mean continuity and mean momentum equations (2.4) and (2.5). Assuming that the mean specific heat is constant, the Reynolds-averaged energy equation (2.6) simplifies to the form

$$\dot{\bar{\rho}}\bar{C}_v\dot{\tilde{T}} = -\overline{p' u'_{i,i}} + \bar{\rho}\varepsilon \quad (2.19)$$

for a compressible homogeneous shear flow at high Reynolds numbers.

The substitution of (2.16) into the contraction of (2.14) yields the turbulent kinetic energy equation

$$\dot{\bar{\rho}}\dot{K} = \bar{\rho}\mathcal{P} + \overline{p' u'_{i,i}} - \bar{\rho}\varepsilon \quad (2.20)$$

where $K \equiv \frac{1}{2}\widetilde{u''_i u''_i}$ is the Favre-averaged turbulent kinetic energy and $\mathcal{P} \equiv -\tau_{12}S$ is the turbulence production. Equation (2.20) can be combined with (2.19) to yield a transport equation for the turbulence Mach number. This transport equation takes the form

$$\dot{M}_t = \frac{M_t}{2K}\mathcal{P} + \frac{M_t}{2\bar{\rho}K} \left[1 + \frac{1}{2}\gamma(\gamma-1)M_t^2 \right] (\overline{p' u'_{i,i}} - \bar{\rho}\varepsilon) \quad (2.21)$$

where $\gamma \equiv \bar{C}_p/\bar{C}_v$ is the ratio of specific heats and $M_t \equiv \sqrt{2K/\gamma R\tilde{T}}$ is the turbulent Mach number. Recently proposed models for the four turbulence correlations that are needed for closure – namely, ε_s , ε_c , $\overline{p' u'_{i,i}}$ and Π_{ij} – will be discussed in the next section.

3. THE TURBULENCE MODELS TO BE TESTED

In almost all existing compressible second-order closures, the deviatoric part of the pressure-strain correlation is modeled as a variable density extension of its incompressible counterpart. Furthermore, as in the majority of incompressible turbulence models, the deviatoric part of the dissipation rate tensor is neglected by invoking the Kolmogorov assumption of local isotropy [18, 19]. This leads to a hierarchy of models that are of the general form:

$$\Pi_{ij} = \bar{\rho}\epsilon_s A_{ij}(b) + \bar{\rho}K M_{ijkl}(b)(\tilde{u}_{k,l} - \frac{1}{3}\tilde{u}_{m,m}\delta_{kl}) \quad (3.1)$$

where

$$b_{ij} = \frac{\tilde{u}_i''\tilde{u}_j'' - \frac{1}{3}\tilde{u}_k''\tilde{u}_k''\delta_{ij}}{\tilde{u}_m''\tilde{u}_m''} \quad (3.2)$$

is the Reynolds stress anisotropy tensor. In (3.1), A_{ij} and M_{ijkl} are identical to their incompressible forms; compressibility effects are only accounted for through changes in the mean density. Since the mean density $\bar{\rho}$ is constant in homogeneous shear flow – and the mean dilatation $\tilde{u}_{i,i}$ is zero – it follows that the hierarchy of pressure-strain models (3.1) is completely identical to its incompressible counterpart. The consequences of this will be discussed later.

In this paper, variable density extensions of three incompressible pressure-strain models will be considered: the Launder, Reece and Rodi [11] model, the Fu, Launder and Tselenidis [12] model and the Speziale, Sarkar and Gatski [13] model. The first model is chosen since it is the most widely used pressure-strain model; the last two models are chosen since they have recently been shown to perform the best among a variety of existing models for incompressible homogeneous shear flow [7, 8]. The detailed form of these models are provided below.

Launder, Reece & Rodi Model

$$\begin{aligned} \Pi_{ij} = & -C_1\bar{\rho}\epsilon_s b_{ij} + \frac{4}{5}\bar{\rho}K \left(\tilde{S}_{ij} - \frac{1}{3}\tilde{S}_{kk}\delta_{ij} \right) + C_2\bar{\rho}K \left(b_{ik}\tilde{S}_{jk} \right. \\ & \left. + b_{jk}\tilde{S}_{ik} - \frac{2}{3}b_{kl}\tilde{S}_{kl}\delta_{ij} \right) + C_3\bar{\rho}K(b_{ik}\tilde{\omega}_{jk} + b_{jk}\tilde{\omega}_{ik}) \end{aligned} \quad (3.3)$$

where

$$\tilde{S}_{ij} = \frac{1}{2}(\tilde{u}_{i,j} + \tilde{u}_{j,i}), \quad \tilde{\omega}_{ij} = \frac{1}{2}(\tilde{u}_{i,j} - \tilde{u}_{j,i}) \quad (3.4)$$

$$C_1 = 3.0, \quad C_2 = 1.75, \quad C_3 = 1.31 \quad (3.5)$$

Fu, Launder & Tslepidakis Model

$$\begin{aligned}
 \Pi_{ij} = & -C_1 \bar{\rho} \epsilon_s b_{ij} + C_2 \bar{\rho} \epsilon_s \left(b_{ik} b_{kj} - \frac{1}{3} b_{kl} b_{kl} \delta_{ij} \right) \\
 & + \frac{4}{5} \bar{\rho} K \left(\tilde{S}_{ij} - \frac{1}{3} \tilde{S}_{kk} \delta_{ij} \right) + 1.2 \bar{\rho} K \left(b_{ik} \tilde{S}_{jk} \right. \\
 & \left. + b_{jk} \tilde{S}_{ik} - \frac{2}{3} b_{kl} \tilde{S}_{kl} \delta_{ij} \right) + \frac{26}{15} \bar{\rho} K (b_{ik} \tilde{\omega}_{jk} \\
 & + b_{jk} \tilde{\omega}_{ik}) + \frac{4}{5} \bar{\rho} K (b_{ik} b_{kl} \tilde{S}_{jl} + b_{jk} b_{kl} \tilde{S}_{il} \\
 & - 2 b_{ik} \tilde{S}_{kl} b_{lj} - 3 b_{kl} \tilde{S}_{kl} b_{ij}) \\
 & + \frac{4}{5} \bar{\rho} K (b_{ik} b_{kl} \tilde{\omega}_{jl} + b_{jk} b_{kl} \tilde{\omega}_{il}) - \frac{14}{5} \bar{\rho} K [8II(b_{ik} \tilde{\omega}_{jk} \\
 & + b_{jk} \tilde{\omega}_{ik})] + 12(b_{ik} b_{kl} \tilde{\omega}_{lm} b_{mj} + b_{jk} b_{kl} \tilde{\omega}_{lm} b_{mi})]
 \end{aligned} \tag{3.6}$$

where

$$C_1 = 2 - 120II F^{1/2} - 2F^{1/2}, \quad C_2 = 144III F^{1/2} \tag{3.7}$$

$$II = -\frac{1}{2} b_{ij} b_{ij}, \quad III = \frac{1}{3} b_{ij} b_{jk} b_{ki} \tag{3.8}$$

$$F = 1 + 9II + 27III \tag{3.9}$$

Speziale, Sarkar & Gatski Model

$$\begin{aligned}
 \Pi_{ij} = & -(C_1 \bar{\rho} \epsilon_s + C_1^* \bar{\rho} \mathcal{P}) b_{ij} + C_2 \bar{\rho} \epsilon_s \left(b_{ik} b_{kj} - \frac{1}{3} b_{kl} b_{kl} \delta_{ij} \right) \\
 & +(C_3 - C_3^* II_b^{1/2}) \bar{\rho} K \left(\tilde{S}_{ij} - \frac{1}{3} \tilde{S}_{kk} \delta_{ij} \right) \\
 & + C_4 \bar{\rho} K \left(b_{ik} \tilde{S}_{jk} + b_{jk} \tilde{S}_{ik} - \frac{2}{3} b_{kl} \tilde{S}_{kl} \delta_{ij} \right) \\
 & + C_5 \bar{\rho} K (b_{ik} \tilde{\omega}_{jk} + b_{jk} \tilde{\omega}_{ik})
 \end{aligned} \tag{3.10}$$

where

$$C_1 = 3.4, \quad C_1^* = 1.80, \quad C_2 = 4.2 \tag{3.11}$$

$$C_3 = \frac{4}{5}, \quad C_3^* = 1.30, \quad C_4 = 1.25 \tag{3.12}$$

$$C_5 = 0.40, \quad II_b = b_{ij} b_{ij}, \quad \mathcal{P} = -\tau_{ij} \dot{u}_{ij}. \tag{3.13}$$

These models will hereafter be referred to as the LRR, FLT and SSG models, respectively.

Since the mean dilatation $\bar{u}_{i,i}$ is zero in homogeneous shear flow, virtually all existing model transport equations for the solenoidal dissipation are of the form [19 - 21]

$$\dot{\epsilon}_s = C_{\epsilon 1} \frac{\epsilon_s}{K} \mathcal{P} - C_{\epsilon 2} \frac{\epsilon_s^2}{K} \quad (3.14)$$

in compressible homogeneous shear flow. This equation is identical to its incompressible counterpart. In (3.14), $\mathcal{P} \equiv -\tau_{12}S$ is the turbulence production and $C_{\epsilon 1}$ and $C_{\epsilon 2}$ are constants (in the SSG model, $C_{\epsilon 1} = 1.44$ and $C_{\epsilon 2} = 1.83$ whereas in the LRR and FLT models, $C_{\epsilon 1} = 1.44$ and $C_{\epsilon 2} = 1.90$). Two recent models for the compressible dissipation will be considered that were proposed by Sarkar *et al* [14] and Zeman [16]. These models are algebraic and of the general form

$$\epsilon_c = f(M_t) \epsilon_s \quad (3.15)$$

where M_t is the turbulence Mach number defined earlier. In the Sarkar *et al* [14] model

$$\epsilon_c = \alpha_1 M_t^2 \epsilon_s \quad (3.16)$$

which is obtained from an asymptotic analysis that is formally valid for small turbulent Mach numbers. The constant α_1 in (3.16) was determined to be approximately 0.5 based on direct numerical simulations of homogeneous turbulence [15]. On the other hand, the compressible dissipation rate model of Zeman [16] is based on an analysis that incorporates the effects of eddy shocklets. For homogeneous shear flow, this model takes the form [20]

$$\epsilon_c = \left\{ 1 - \exp(-[(M_t - 0.25)/0.8]^2) \right\} \epsilon_s \quad (3.17)$$

for $M_t \geq 0.25$; $\epsilon_c = 0$ for $M_t < 0.25$.

The pressure-dilatation model that we will primarily consider is that due to Sarkar [15]. This model is algebraic and takes the following simple form in homogeneous shear flow:

$$\overline{p' u'_{i,i}} = -\alpha_2 \bar{\rho} \mathcal{P} M_t + \alpha_3 \bar{\rho} \epsilon_s M_t^2 \quad (3.18)$$

where α_2 and α_3 are constants that take on the values of 0.15 and 0.2, respectively. Some limited comparisons will also be made with the pressure-dilatation model of Zeman [17] which is given by

$$\overline{p' u'_{i,i}} = (\bar{p}\gamma)^{-1} \left[\frac{\bar{p}^2 - p_e^2}{\tau_f} + \left(\frac{5 - 3\gamma}{12} \right) \bar{p}^2 \bar{u}_{i,i} \right] = -\frac{1}{2} \frac{d}{dt} \left(\bar{p}^2 / \gamma \bar{p} \right) \quad (3.19)$$

where

$$\tau_f = 0.4 \frac{K}{\epsilon} M_t \quad (3.20)$$

and

$$p_e^2 = 2\bar{\rho}^2 K \gamma R \tilde{T} \left(\frac{M_t^2 + M_t^4}{1 + M_t^2 + M_t^4} \right). \quad (3.21)$$

Of course, in (3.19), $\bar{p} \equiv \bar{\rho}R\tilde{T}$ and $\bar{u}_{i,i} = 0$ for homogeneous shear flow. In the next section, a comparison of computed results obtained from these models for compressible homogeneous shear flow will be made.

4. DISCUSSION OF RESULTS

The transport equations (2.6), (2.14) and (3.14) – incorporating the models discussed in Section 3 – were solved numerically for compressible homogeneous shear flow using a fourth-order accurate Runge-Kutta numerical integration scheme. Comparisons will be made with the direct numerical simulations (DNS) of compressible homogeneous shear flow by Blaisdell *et al* [3]. Both time-evolving fields and equilibrium states will be compared with DNS results. Comparisons will be made with run SHA 192 of Blaisdell *et al* [3] since it is the best resolved run that is of long duration (until $St \approx 24$). It will be shown that, consistent with the DNS, the models predict that the turbulent kinetic energy, turbulent dissipation rate and mean temperature grow exponentially with time. All structural parameters such as the anisotropy tensor b_{ij} and turbulent Mach number M_t achieve equilibrium values that are independent of the initial conditions.

First, we will consider model predictions for the case where there are no explicit dilatational terms. This is done for one major reason: until very recently, the vast majority of Reynolds stress calculations of compressible turbulent shear flows were conducted with variable density extensions of incompressible models where explicit turbulent dilatational terms were not included. Consequently, a benchmark is established for assessing the performance of the recently proposed dilatational models. In Figure 1, the time evolution of the turbulent kinetic energy predicted by variable density extensions of the LRR, FLT and SSG models – with compressible dissipation and pressure-dilatation effects neglected – are compared with DNS results of Blaisdell *et al* [3] (run SHA 192). Here, $K^* \equiv K/K_0$ and $t^* \equiv St$ are the dimensionless turbulent kinetic energy and the dimensionless time, respectively, where a subscript 0 denotes the initial value. From these results, it is clear that all of the models drastically overpredict the growth rate of the turbulent kinetic energy – a deficiency that arises from the complete neglect of turbulent dilatational effects as discussed by previous authors [14, 15, 19]. In Figures 2-3, the model predictions for the time evolution of the turbulent dissipation rate ($\epsilon^* = \epsilon/\epsilon_0$) and turbulent Mach number (M_t) are displayed. Here, as with the results shown in Figure 1 for the turbulent kinetic energy, the calculations are made for $St \geq 2$ in order to avoid the unphysical early transient of the DNS which lasts for

approximately one eddy turnover time due to the fact that the flow is initially seeded with an artificial random Gaussian field. It is obvious from these results that the models substantially overpredict the turbulent dissipation rate and turbulent Mach number. In regard to the latter, highly unphysical equilibrium turbulence Mach numbers greater than 1.5 are predicted. This is true for both the FLT and SSG models which yield excellent predictions for incompressible homogeneous shear flow. Consequently, it is clear that *variable density extensions of incompressible Reynolds stress models, with turbulent dilatational effects neglected, cannot properly describe compressible homogeneous shear flow* – a conclusion consistent with previous findings. The compressible dissipation and pressure-dilatation correlation give rise to a significant reduction in the growth rate of the turbulent kinetic energy for compressible homogeneous shear flow.

In Figure 4, computed results for the turbulent kinetic energy obtained from the LRR, FLT and SSG models – with the compressible dissipation and pressure-dilatation models of Sarkar *et al* [14, 15] – are compared with DNS results. With the addition of these turbulent dilatational terms, the FLT and SSG models are now able to properly predict the reduced growth rate of the turbulent kinetic energy that arises from compressibility effects in homogeneous shear flow. The LRR model overpredicts the growth rate of the turbulent kinetic energy by an amount comparable to that which has been documented for incompressible homogeneous shear flow (Speziale, Gatski and Mac Giolla Mhuiris [7] showed that the LRR model overpredicts the growth rate by about 25% for the incompressible case). The computed time evolutions of the turbulent dissipation rate are compared with DNS results in Figure 5. Although the dissipation rate is overpredicted, the inclusion of the dilatational models of Sarkar leads to a substantial improvement over the results shown in Figure 2. The computed model predictions for the time evolution of the turbulence Mach number are compared with DNS results in Figure 6. With the addition of the dilatational models of Sarkar, the FLT and SSG models now yield remarkably good predictions for the turbulence Mach number as illustrated by these results.

Computed results for the LRR, FLT and SSG models with the addition of the compressible dissipation and pressure-dilatation models of Zeman [16, 17] will now be considered. Model predictions for the time evolution of the turbulent kinetic energy, turbulent dissipation rate and turbulent Mach number are compared with DNS results in Figures 7-9. Most notably, the predictions of the FLT and SSG models for the turbulent kinetic energy and turbulent Mach number are comparably good to those obtained using the dilatational models of Sarkar. Alternative tests of the Zeman models were recently reported for compressible homogeneous shear flow that are comparably favorable [22].

In Figures 10(a)-10(c), computed results for the independent non-vanishing components

of the Reynolds stress anisotropy tensor obtained from the LRR, FLT and SSG models – using the dilatational models of Sarkar – are compared with DNS results. It is clear from these results that all of the models drastically underpredict the magnitude of the normal Reynolds stress anisotropies in compressible homogeneous shear flow; on the other hand, the models overpredict the magnitude of the Reynolds shear stress anisotropy. The DNS results of Blaisdell *et al* [3] indicate that the normal Reynolds stress anisotropies in compressible homogeneous shear flow are nearly twice as large as their incompressible counterparts [23]; the magnitude of the Reynolds shear stress anisotropy is approximately 25% lower for compressible homogeneous shear flow. Even with the addition of what appear to be reasonably sound models for the compressible dissipation and pressure dilatation, variable density extensions of the LRR, FLT and SSG models are unable to predict the dramatic changes in the Reynolds stress anisotropies that arise from compressible effects. This can be seen more clearly from Tables 1-3 where the model predictions for the equilibrium Reynolds stress anisotropies are compared with DNS results for incompressible homogeneous shear flow and for compressible homogeneous shear flow, wherein both the dilatational models of Sarkar and Zeman are implemented. It is obvious from these results that the individual model predictions are in reasonably close range for both compressible and incompressible homogeneous shear flow whereas the DNS results are drastically different.

5. CONCLUSION

A systematic evaluation of recently proposed Reynolds stress turbulence closures for high-speed compressible flows has been conducted with the use of the DNS data base of Blaisdell *et al* [3] for compressible homogeneous shear flow. The recently developed dilatational models of Sarkar *et al* [14, 15] and Zeman [16, 17] were tested in conjunction with variable density extensions of two of the newest models for the pressure-strain correlation: the Fu, Launder and Tslepidakis (FLT) model and the Speziale, Sarkar and Gatski (SSG) model. Consistent with the findings of earlier studies, it was found that when dilatational effects arising from the compressible dissipation and the pressure-dilatation correlation are neglected, variable density extensions of existing Reynolds stress turbulence closures yield poor predictions for compressible homogeneous shear flow. DNS results indicate that compressibility effects lead to a substantial reduction in the growth rate of the turbulent kinetic energy – a feature that cannot be predicted by Reynolds stress turbulence closures wherein turbulent dilatational terms are neglected. With the addition of the compressible dissipation and pressure-dilatation models of Sarkar and Zeman, the newest Reynolds stress turbulence closures are able to accurately predict the reduction in the growth rate of the turbulent kinetic energy. Accurate results are also obtained for the turbulent Mach number which is

overpredicted by 100% when turbulent dilatational terms are neglected. There appears to be little doubt these dilatational models represent significant progress in the modeling of compressible homogeneous turbulence.

Although the inclusion of the newest compressible dissipation and pressure-dilatation models in Reynolds stress turbulence closures leads to substantially improved predictions for the turbulent kinetic energy and Mach number, some substantial deficiencies still remain for the proper description of compressible homogeneous shear flow. DNS results indicate that compressibility effects in homogeneous shear flow lead to a substantial modification of the equilibrium Reynolds stress anisotropies wherein the magnitude of the normal components are nearly doubled and the magnitude of the shear component is reduced by approximately 25%. Even when compressible dissipation and pressure-dilatation models are added, the Reynolds stress turbulence closures considered in this study are still unable to predict this effect. This is due to deficiencies in the modeling of the deviatoric part of the pressure-strain correlation which controls the level of Reynolds stress anisotropy. The pressure-strain models considered herein – as well as those used in virtually all previous studies of compressible turbulence – do not account for explicit compressible effects. This is a reasonable approximation for compressible flows where the turbulent Mach number $M_t < 0.3$: a restriction that allows for the Morkovin [24] hypothesis to be invoked. However, in compressible homogeneous shear flow the turbulence Mach number achieves an equilibrium value of approximately 0.6 – a value that is too large to neglect explicit compressible effects in the modeling of the pressure-strain correlation. The standard hierarchy of pressure-strain models is based on an analysis of the incompressible Poisson equation for the pressure that does not apply to high-speed compressible flows. For these flows, the pressure is determined from a thermodynamic equation of state unlike the pressure in incompressible flows which is a Lagrange multiplier determined by the solenoidal constraint on the velocity field. If high-speed turbulent shear flows are to be better described, entirely new models are needed for the deviatoric part of the pressure-strain correlation that incorporate some compressible turbulence physics.

ACKNOWLEDGEMENTS

The first author (CGS) acknowledges the partial support of the Center for Turbulence Research (Stanford University) through its visitors program. The second author (RA) was supported by the National Aeronautics and Space Administration under NASA Contract NAS1-19299. Helpful comments by Dr. Otto Zeman on his dilatational models are gratefully acknowledged.

References

- [1] T. Passot and A. Pouquet, *Numerical Simulation of Compressible Homogeneous Flows in the Turbulent Regime*, J. Fluid Mech. **181**, 441-446 (1987).
- [2] S. K. Lele, *Compressibility Effects on Turbulence*, Annual Rev. Fluid Mech. **26**, 211-254 (1994).
- [3] G. A. Blaisdell, N. N. Mansour and W. C. Reynolds, *Numerical Simulation of Compressible Homogeneous Turbulence*, J. Fluid Mech. (in press).
- [4] S. Sarkar, G. Erlebacher and M. Y. Hussaini, *Direct Simulation of Compressible Turbulence in a Shear Flow*, Theoret. Comput. Fluid Dynamics **2**, 291-305 (1991).
- [5] S. Sarkar, G. Erlebacher and M. Y. Hussaini, *Compressible Homogeneous Shear: Simulation and Modeling*, Turbulent Shear Flows **8**, pp. 249-267, Springer-Verlag (1993).
- [6] C. G. Speziale and N. Mac Giolla Mhuiris, *On the Prediction of Equilibrium States in Homogeneous Turbulence*, J. Fluid Mech. **209**, 591-615 (1989).
- [7] C. G. Speziale, T. B. Gatski and N. Mac Giolla Mhuiris, *A Critical Comparison of Turbulence Models for Homogeneous Shear Flows in a Rotating Frame*, Phys. Fluids A **2**, 1678-1684 (1990).
- [8] R. Abid and C. G. Speziale, *Predicting Equilibrium States with Reynolds Stress Closures in Channel Flow and Homogeneous Shear Flow*, Phys. Fluids A **5**, 1776-1782 (1993).
- [9] P. Moin, W. C. Reynolds and J. Kim, eds., *Studying Turbulence Using Numerical Simulation Databases - III*, Center for Turbulence Research, Stanford University (1990).
- [10] P. Moin, W. C. Reynolds and J. Kim, eds., *Studying Turbulence Using Numerical Simulation Databases - IV*, Center for Turbulence Research, Stanford University (1992).
- [11] B. E. Launder, G. J. Reece and W. Rodi, *Progress in the Development of a Reynolds Stress Turbulence Closure*, J. Fluid Mech. **68**, 537-566 (1975).
- [12] S. Fu, B. E. Launder and D. P. Tselepidakis, *Accommodating the Effects of High Strain Rates in Modeling the Pressure-Strain Correlation*, UMIST Technical Report TFD/87/5 (1987).
- [13] C. G. Speziale, S. Sarkar and T. B. Gatski, *Modeling the Pressure-Strain Correlation of Turbulence: An Invariant Dynamical Systems Approach*, J. Fluid Mech. **227**, 245-272 (1991).

- [14] S. Sarkar, G. Erlebacher, M. Y. Hussaini and H. O. Kreiss, *The Analysis and Modeling of Dilatational Terms in Compressible Turbulence*, J. Fluid Mech. **227**, 473-493 (1991).
- [15] S. Sarkar, *The Pressure-Dilatation Correlation in Compressible Flows*, Phys. Fluids A **4**, 2674-2682 (1992).
- [16] O. Zeman, *Dilatational Dissipation: The Concept and Application in Modeling Compressible Mixing Layers*, Phys. Fluids A **2**, 178-188 (1990).
- [17] O. Zeman, *Compressible Turbulent Flows: Modeling and Similarity Considerations*, in Annual Research Briefs 1990 – Center for Turbulence Research, pp. 11-22, (P. Moin, W. C. Reynolds and J. Kim, eds.), Stanford University (1990).
- [18] J. O. Hinze, *Turbulence*, McGraw-Hill (1975).
- [19] C. G. Speziale and S. Sarkar, *Second-Order Closure Models for Supersonic Turbulent Flows*, AIAA Paper No. 91-0217 (1991).
- [20] O. Zeman, *Toward a Constitutive Relation in Compressible Turbulence*, in Studies in Turbulence, pp. 285-296, (T. B. Gatski, S. Sarkar and C. G. Speziale, eds.), Springer-Verlag (1992).
- [21] J. P. Dussauge and J. Gaviglio, *The Rapid Expansion of a Supersonic Turbulent Flow: Role of Bulk Dilatation*, J. Fluid Mech. **174**, 81-112 (1987).
- [22] G. A. Blaisdell and O. Zeman, *Investigation of the Dilatational Dissipation in Compressible Homogeneous Shear Flow*, in Studying Turbulence Using Numerical Simulation Databases - IV, pp. 231-245, (P. Moin, W. C. Reynolds and J. Kim, eds.), Center for Turbulence Research, Stanford University (1992).
- [23] M. M. Rogers, P. Moin and W. C. Reynolds, *The Structure and Modeling of the Hydrodynamic and Passive Scalar Fields in Homogeneous Turbulent Shear Flow*, Stanford University Technical Report TF-25 (1986).
- [24] M. Morkovin, *Effects of Compressibility on Turbulent Flows*, in Mecanique de la Turbulence, CNRS, pp. 367-380, (A. Favre, ed.), Gordon & Breach (1964).

Equilibrium Values	LRR Model	FLT Model	SSG Model	DNS Data
b_{11}	0.155	0.208	0.219	0.215
b_{12}	-0.187	-0.146	-0.164	-0.158
b_{22}	-0.121	-0.144	-0.146	-0.153
b_{33}	-0.034	-0.064	-0.073	-0.062

Table 1. Comparison of the model predictions for the equilibrium Reynolds stress anisotropies with the DNS results of Rogers *et al* [23] for incompressible homogeneous shear flow.

Equilibrium Values	LRR Model	FLT Model	SSG Model	DNS Data
b_{11}	0.166	0.189	0.230	0.424
b_{12}	-0.187	-0.148	-0.165	-0.118
b_{22}	-0.130	-0.138	-0.148	-0.236
b_{33}	-0.036	-0.051	-0.082	-0.188

Table 2. Comparison of the compressible model predictions (using the dilatational terms of Sarkar *et al* [14, 15]) for the equilibrium Reynolds stress anisotropies with the DNS results of Blaisdell *et al* [3] for the compressible homogeneous shear flow.

Equilibrium Values	LRR Model	FLT Model	SSG Model	DNS Data
b_{11}	0.167	0.187	0.231	0.424
b_{12}	-0.191	-0.148	-0.167	-0.118
b_{22}	-0.131	-0.137	-0.148	-0.236
b_{33}	-0.036	-0.050	-0.083	-0.188

Table 3. Comparison of the compressible model predictions (using the dilatational terms of Zeman [16, 17]) for the equilibrium Reynolds stress anisotropies with the DNS results of Blaisdell *et al* [3] for compressible homogeneous shear flow.

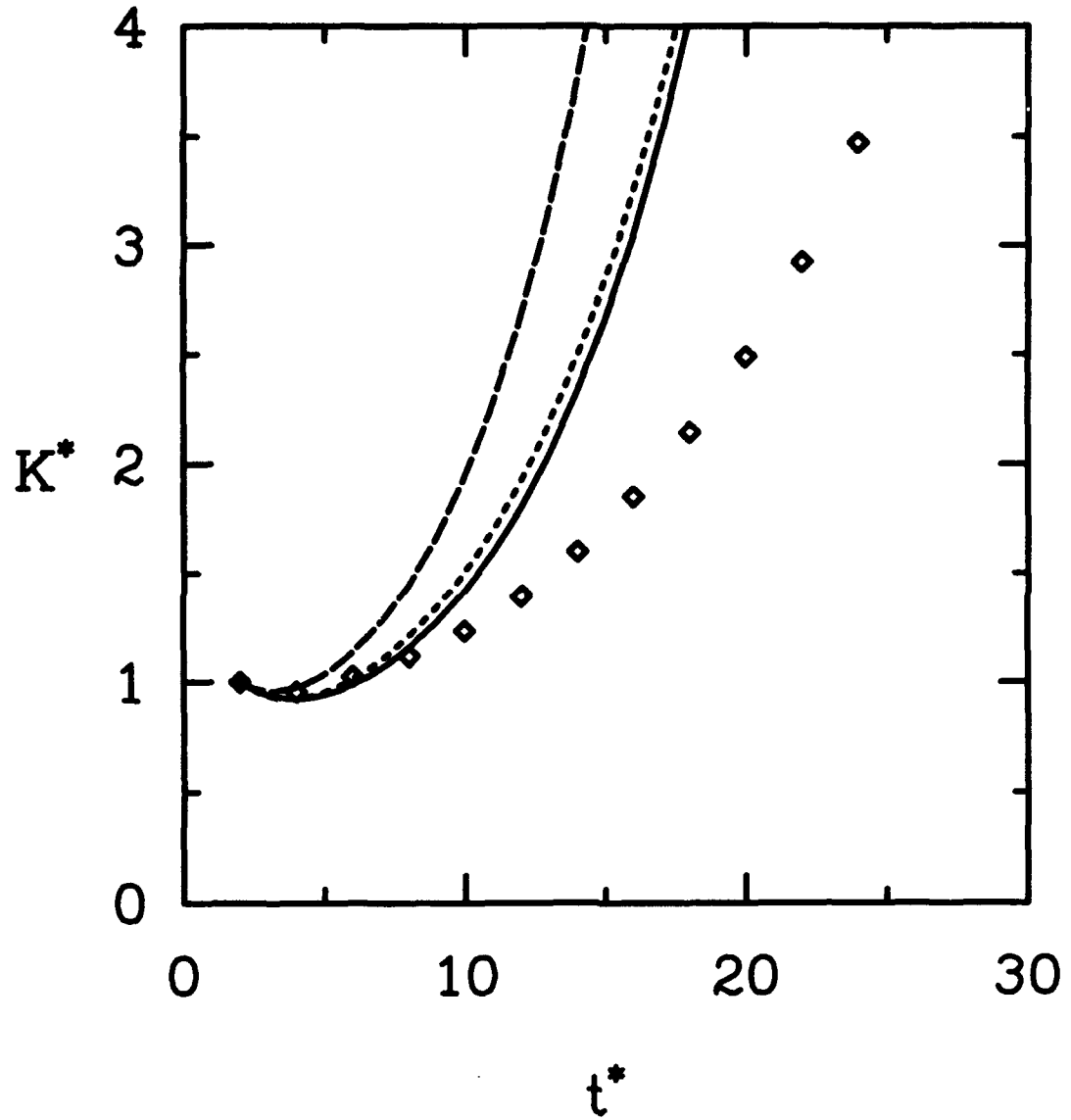


Figure 1. Time evolution of the turbulent kinetic energy: Comparison of the model predictions (without explicit dilatational terms) and the DNS results of Blaisdell *et al* [3] for compressible homogeneous shear flow. (— —) LRR Model; (---) FLT Model; (—) SSG Model; (\diamond) DNS results.

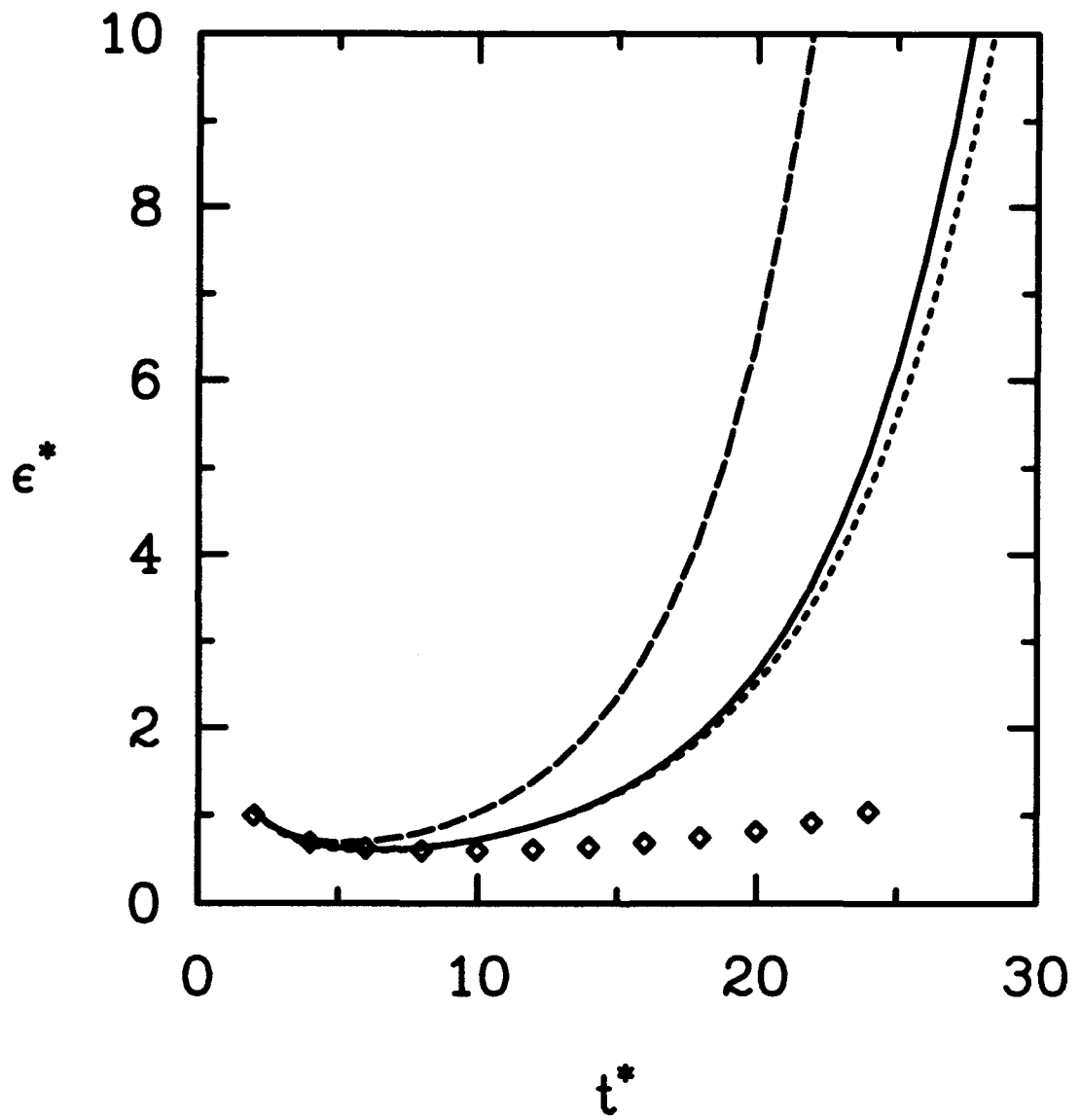


Figure 2. Time evolution of the turbulent dissipation rate: Comparison of the model predictions (without explicit dilatational terms) and the DNS results of Blaisdell *et al* [3] for compressible homogeneous shear flow. (—) LRR Model; (- - -) FLT Model; (—) SSG Model; (\diamond) DNS results.

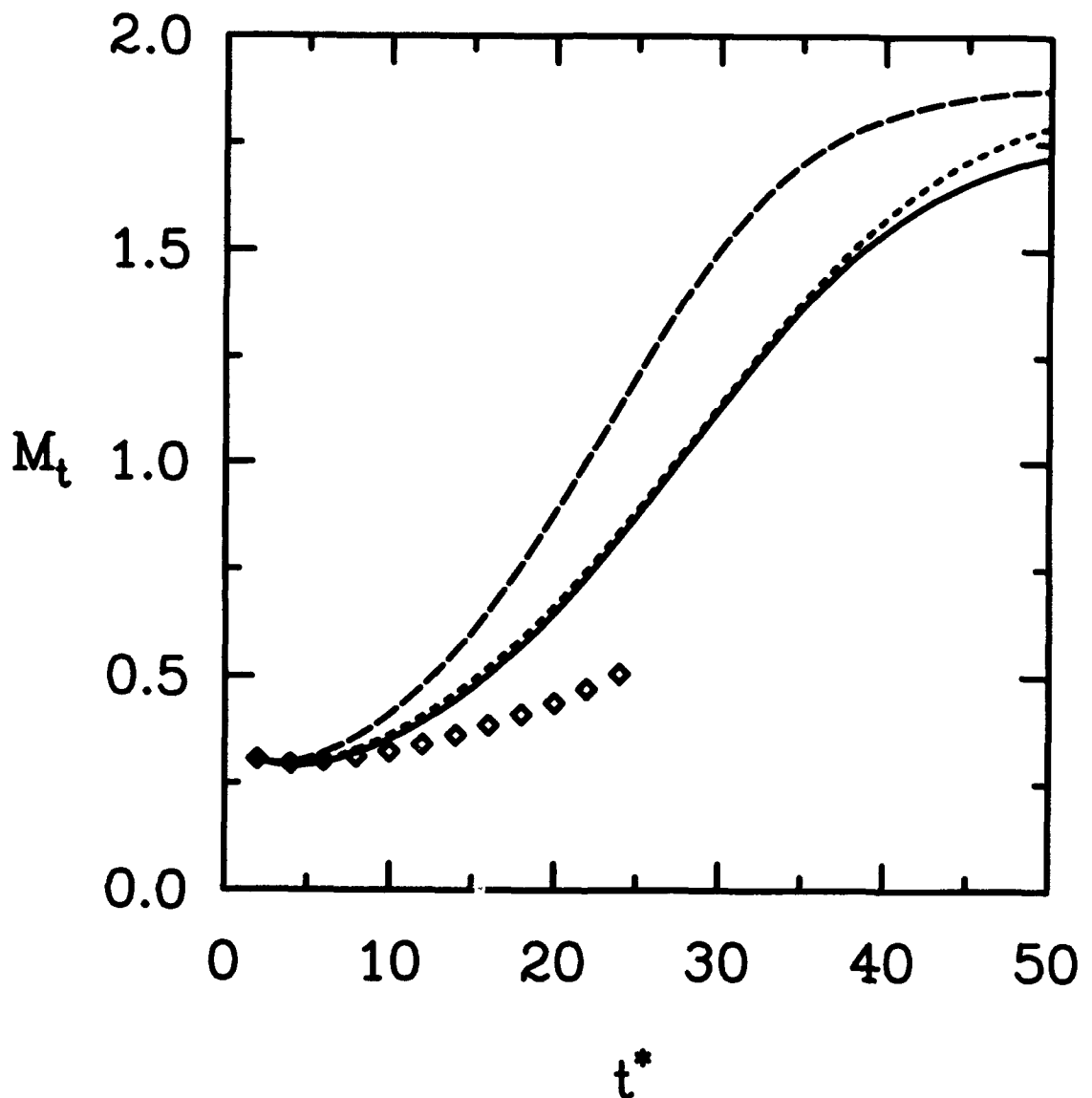


Figure 3. Time evolution of the turbulent Mach number: Comparison of the model predictions (without explicit dilatational terms) and the DNS results of Blaisdell *et al* [3] for compressible homogeneous shear flow. (— —) LRR Model; (- - -) FLT Model; (—) SSG Model; (\diamond) DNS results.

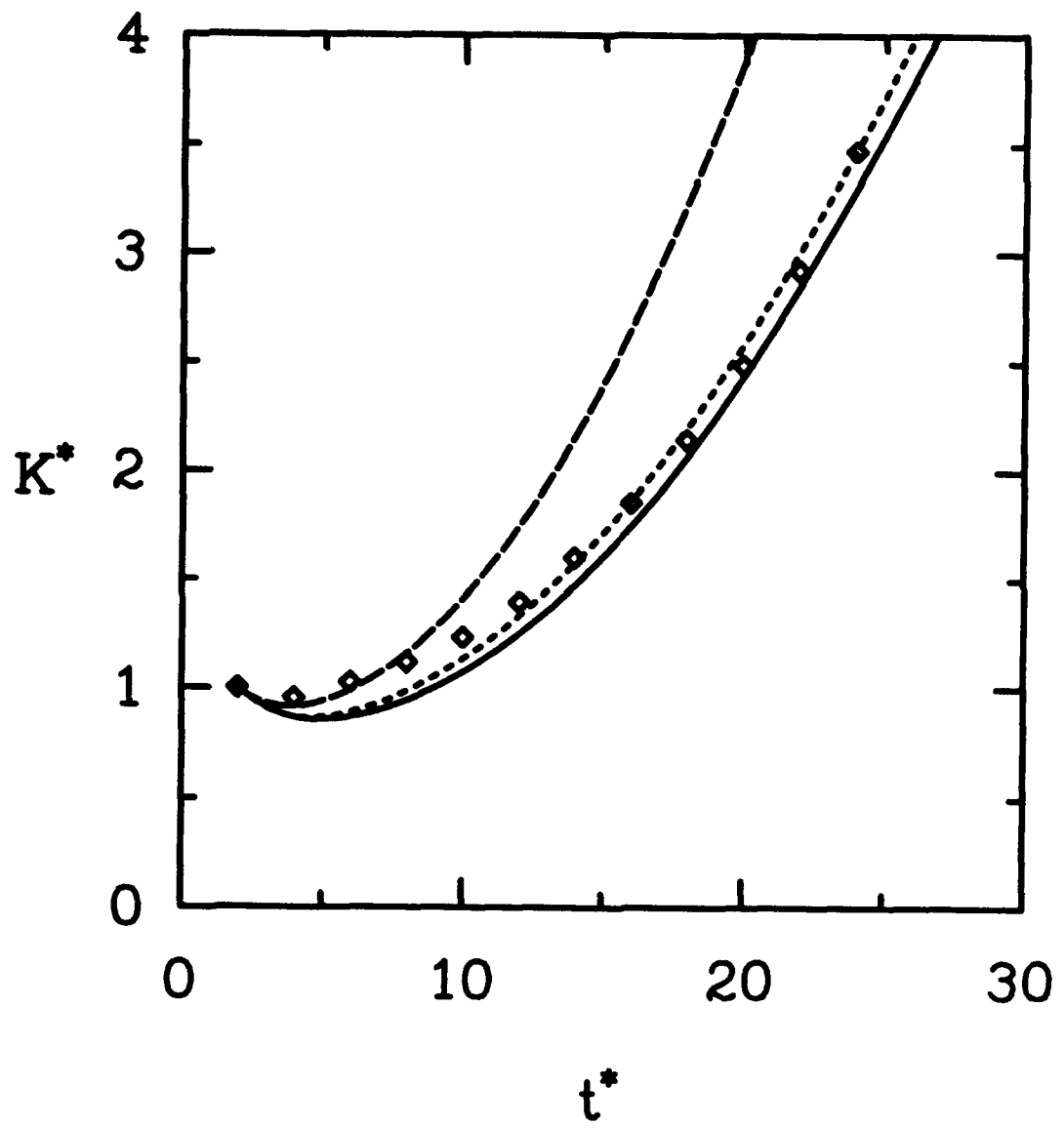


Figure 4. Time evolution of the turbulent kinetic energy: Comparison of the model predictions (with the dilatational terms of Sarkar *et al* [14, 15]) and the DNS results of Blaisdell *et al* [3] for compressible homogeneous shear flow. (— —) LRR Model; (- - -) FLT Model; (—) SSG Model; (\diamond) DNS results.

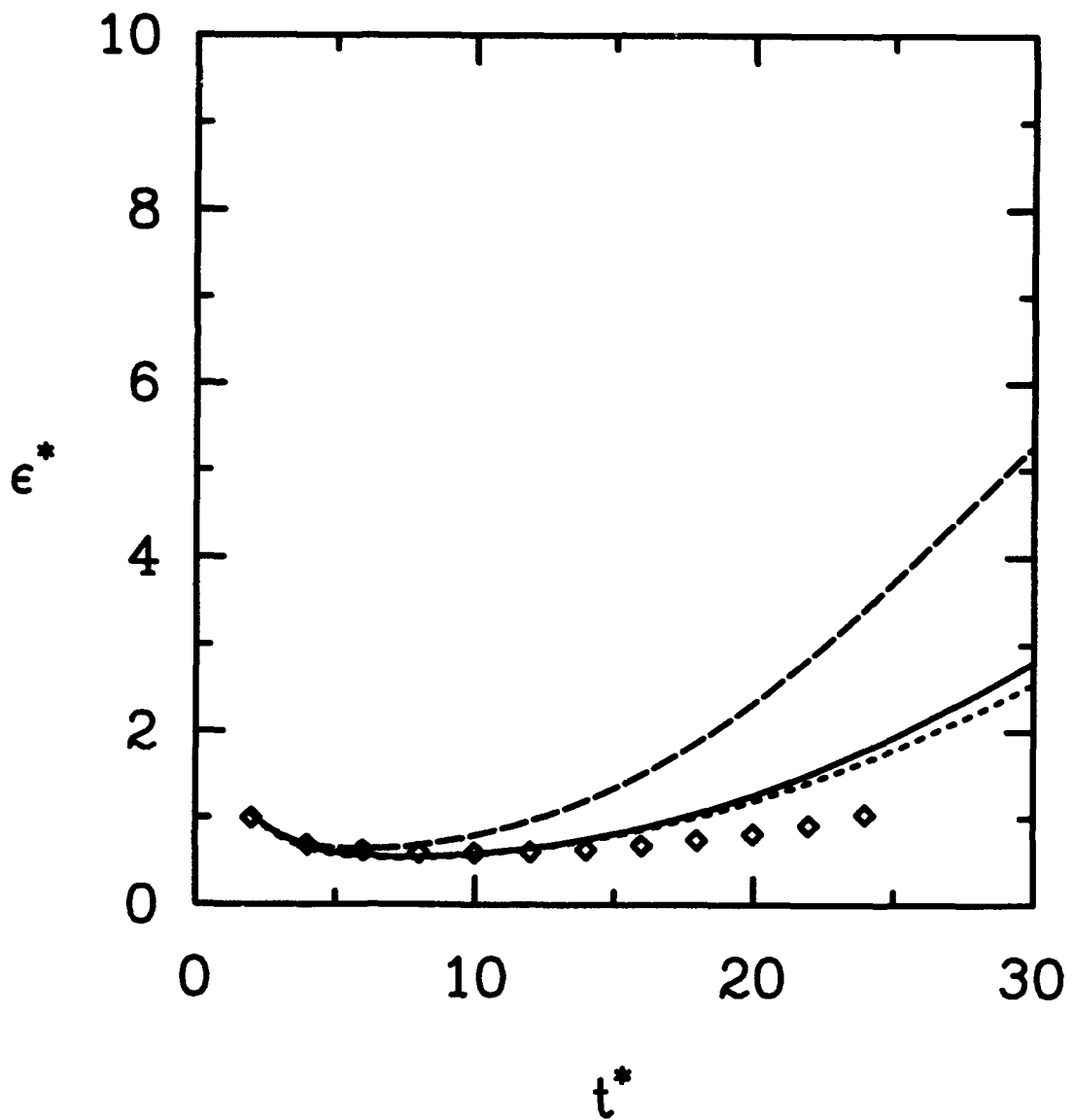


Figure 5. Time evolution of the turbulent dissipation rate: Comparison of the model predictions (with the dilatational terms of Sarkar *et al* [14, 15]) and the DNS results of Blaisdell *et al* [3] for compressible homogeneous shear flow. (—) LRR Model; (- - -) FLT Model; (—) SSG Model; (\diamond) DNS results.

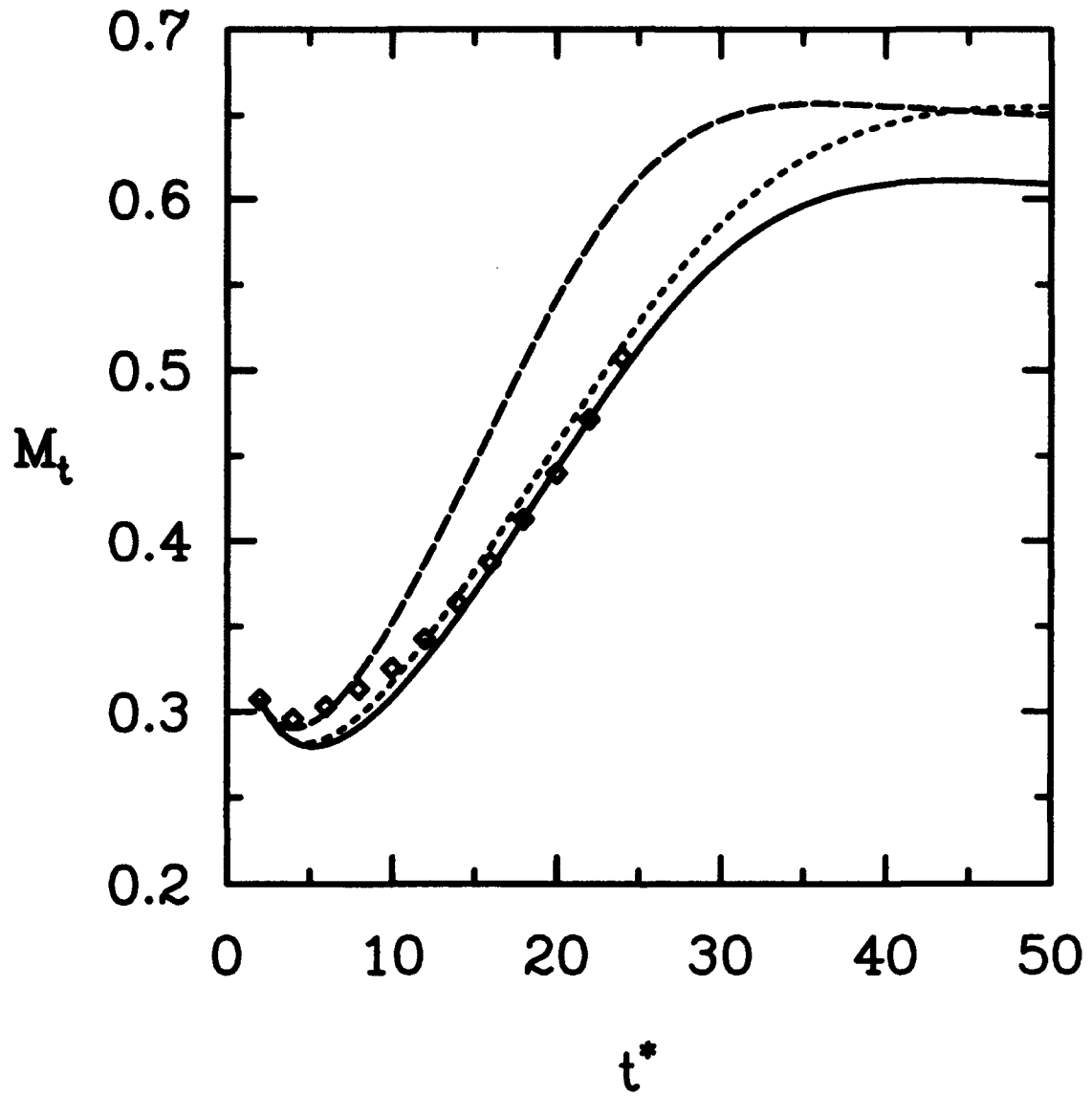


Figure 6. Time evolution of the turbulent Mach number: Comparison of the model predictions (with the dilatational terms of Sarkar *et al* [14, 15]) and the DNS results of Blaisdell *et al* [3] for compressible homogeneous shear flow. (— —) LRR Model; (---) FLT Model; (—) SSG Model; (\diamond) DNS results.

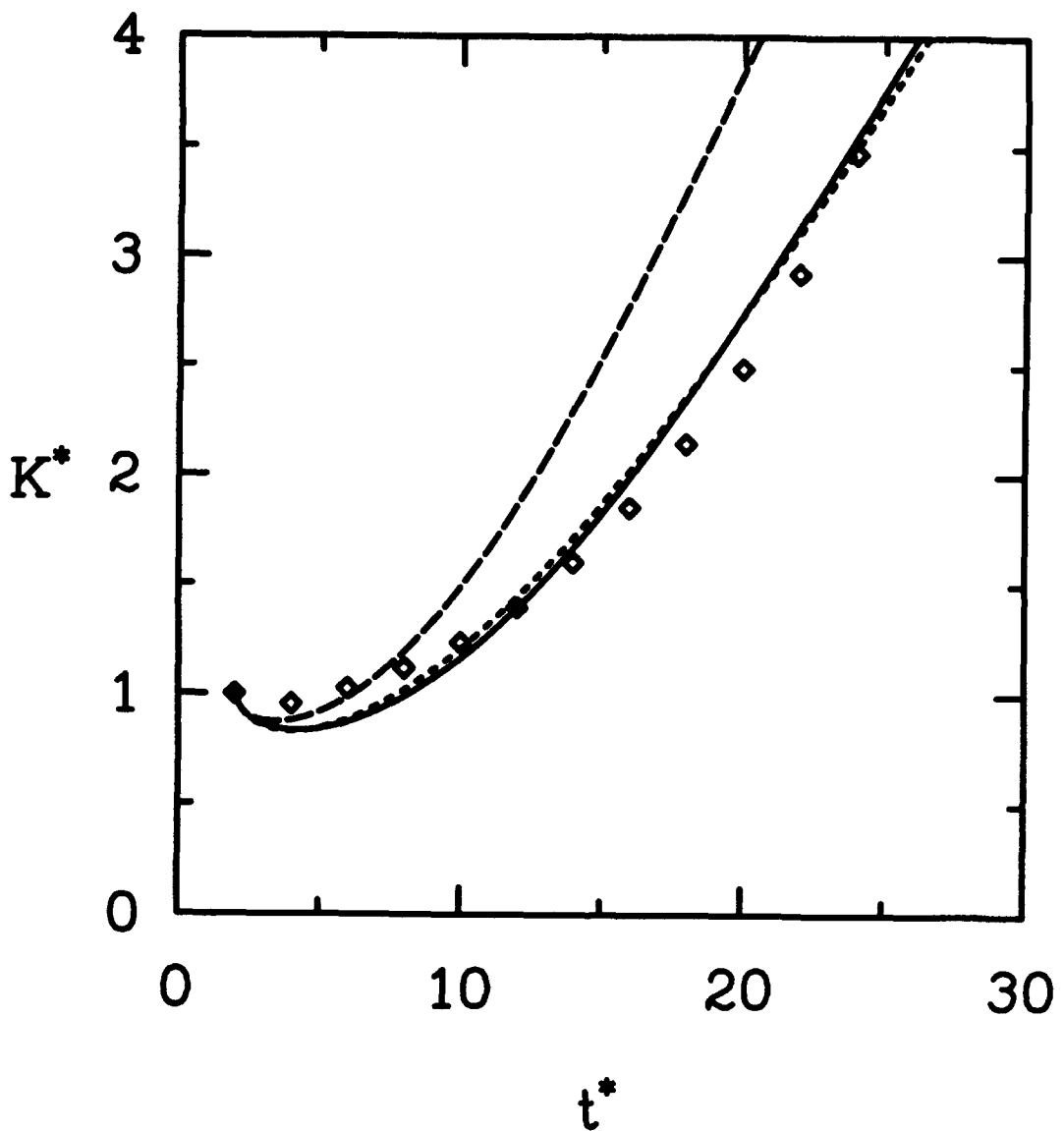


Figure 7. Time evolution of the turbulent kinetic energy: Comparison of the model predictions (with the dilatational terms of Zeman [16, 17]) and the DNS results of Blaisdell *et al* [3] for compressible homogeneous shear flow. (—) LRR Model; (- - -) FLT Model; (—) SSG Model; (\diamond) DNS results.

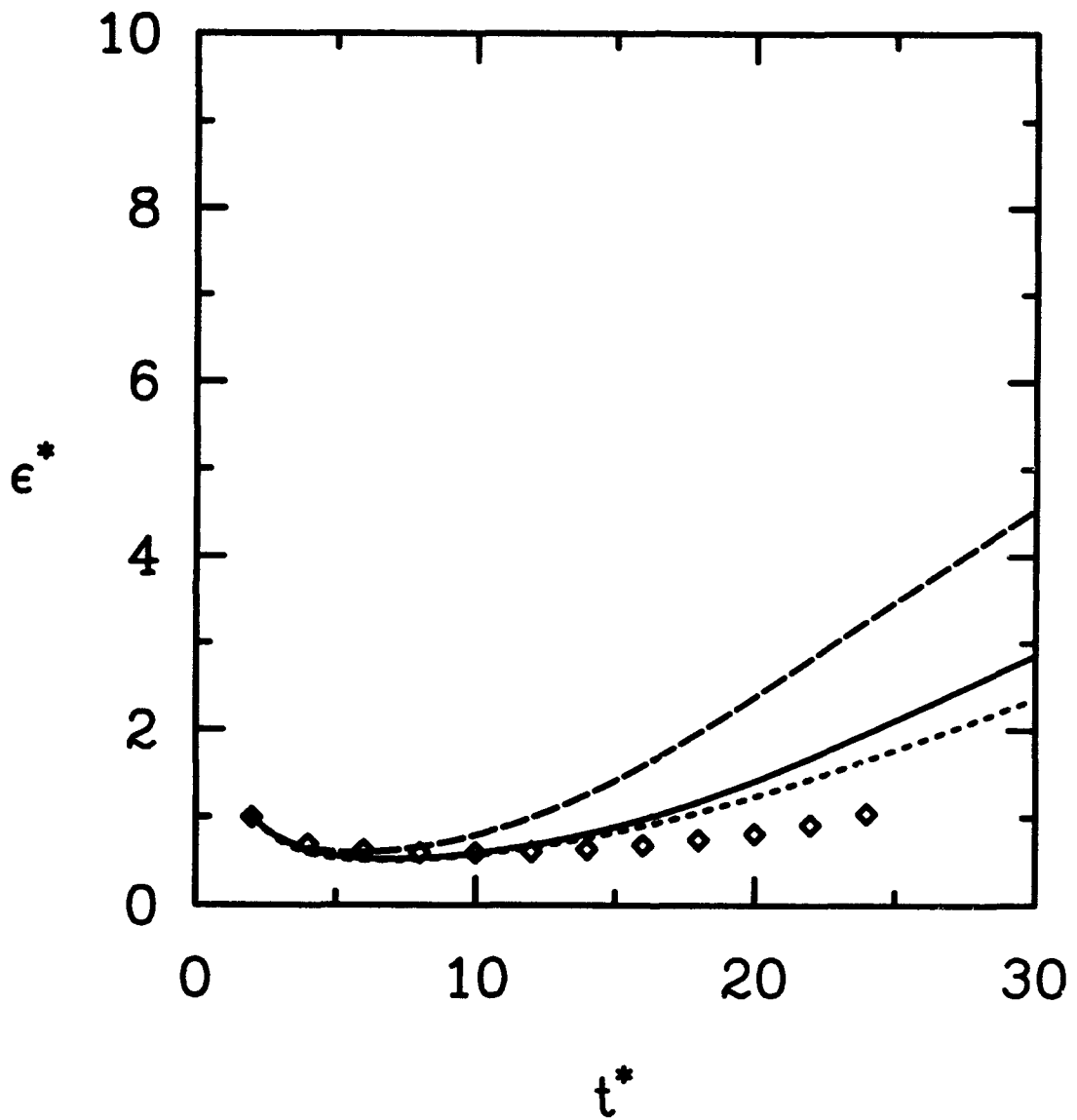


Figure 8. Time evolution of the turbulent dissipation rate: Comparison of the model predictions (with the dilatational terms of Zeman [16, 17]) and the DNS results of Blaisdell *et al* [3] for compressible homogeneous shear flow. (— —) LRR Model; (- - -) FLT Model; (—) SSG Model; (\diamond) DNS results.

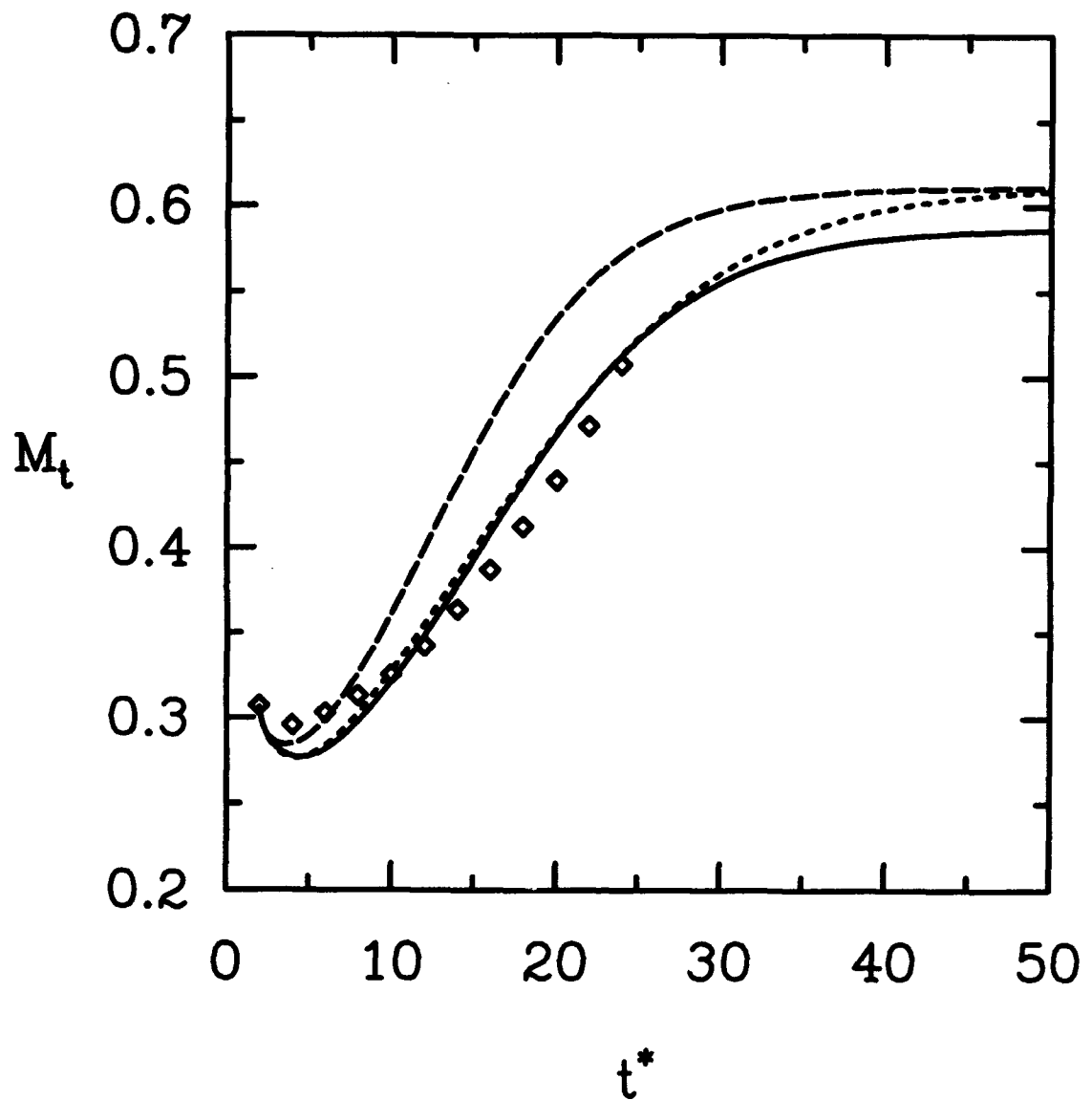


Figure 9. Time evolution of the turbulent Mach number: Comparison of the model predictions (with the dilatational terms of Zeman [16, 17]) and the DNS results of Blaisdell *et al* [3] for compressible homogeneous shear flow. (— —) LRR Model; (---) FLT Model; (—) SSG Model; (\diamond) DNS results.

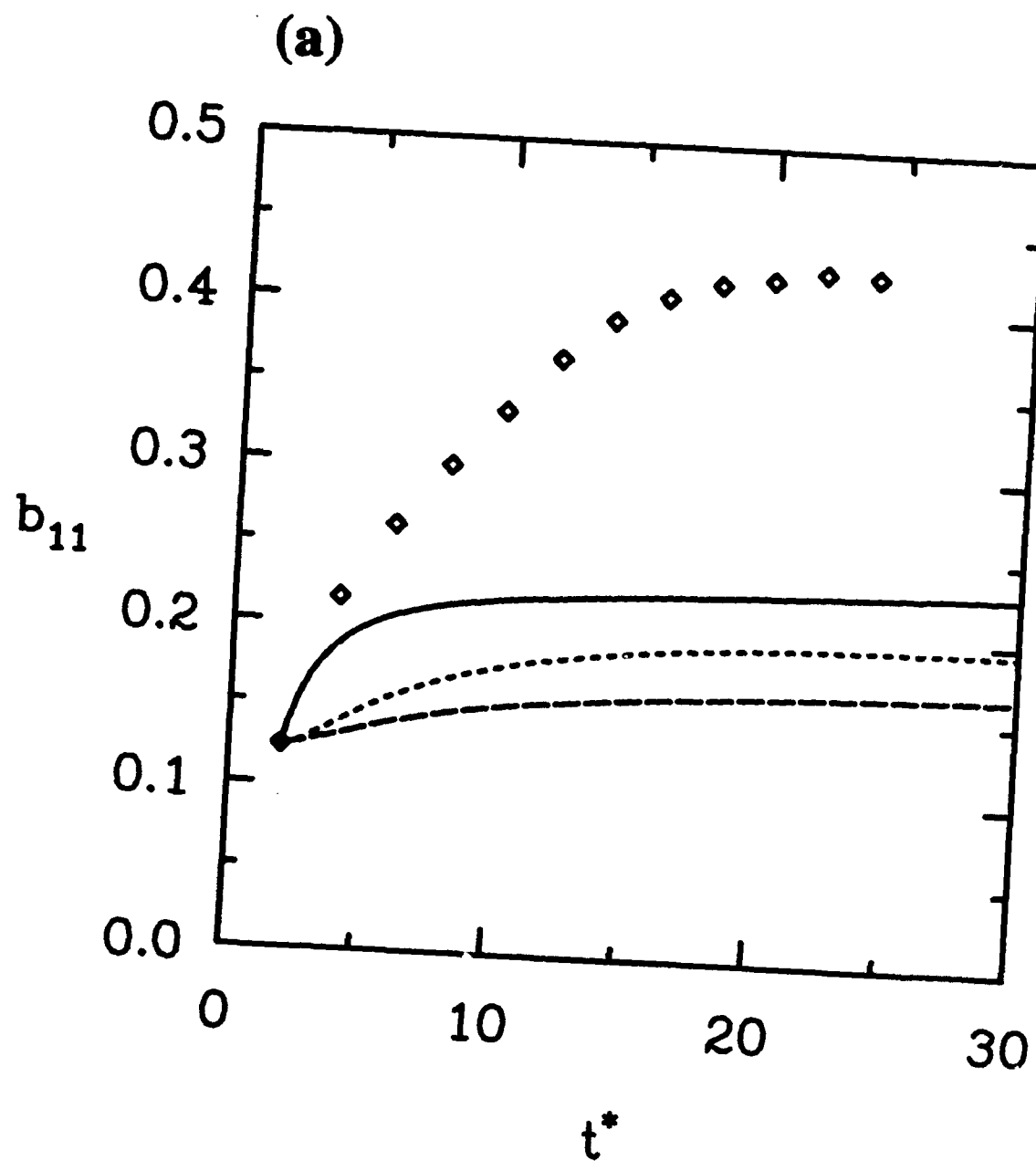


Figure 10. Time evolution of the Reynolds stress anisotropies: Comparison of the model predictions (with the dilatational terms of Sarkar *et al* [14, 15]) and the DNS results of Blaisdell *et al* [3] for compressible homogeneous shear flow. (— —) LRR Model; (- - -) FLT Model; (—) SSG Model; (\diamond) DNS results. (a) b_{11} , (b) b_{22} and (c) b_{12} .

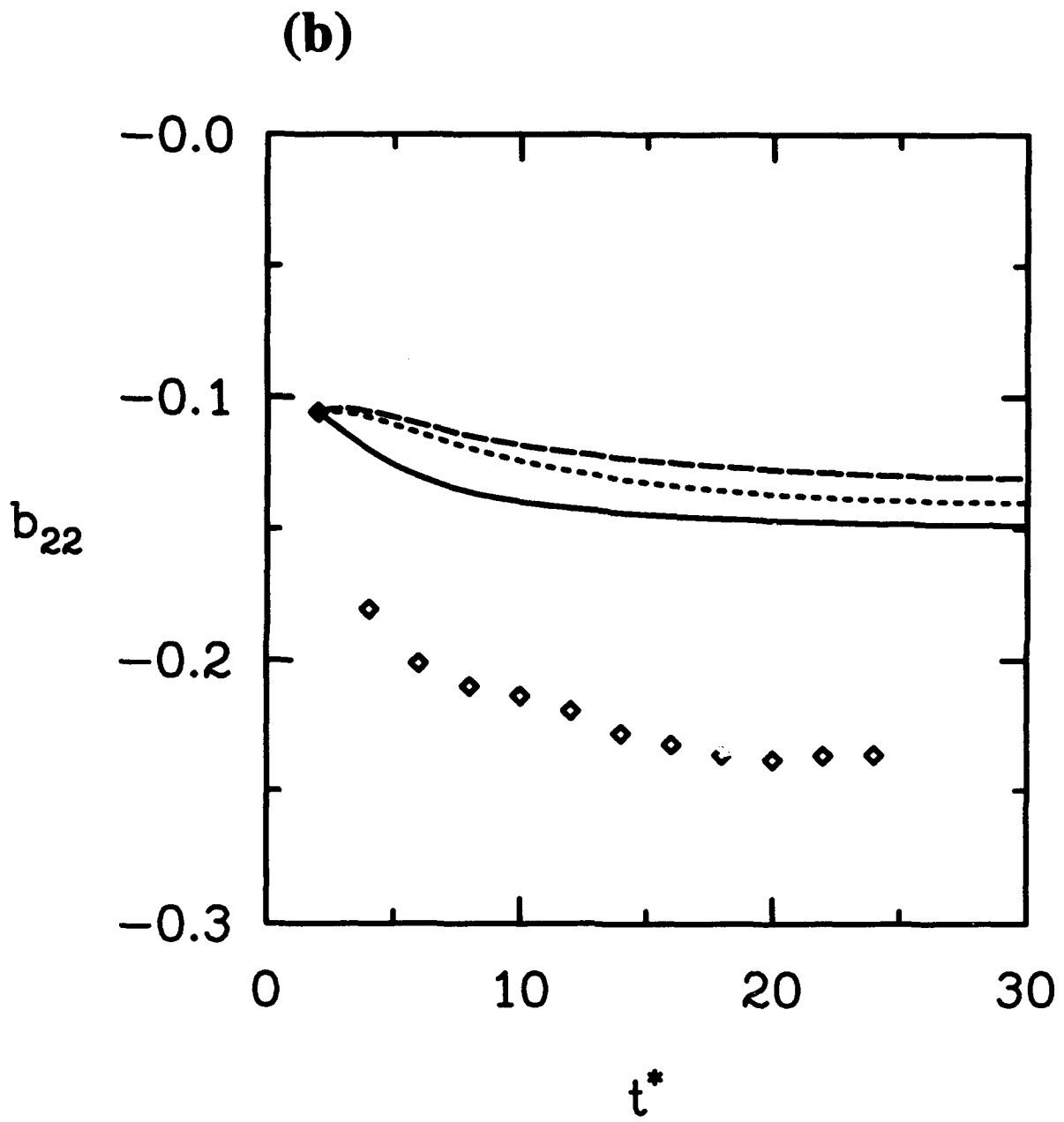


Figure 10. Time evolution of the Reynolds stress anisotropies: Comparison of the model predictions (with the dilatational terms of Sarkar *et al* [14, 15]) and the DNS results of Blaisdell *et al* [3] for compressible homogeneous shear flow. (— —) LRR Model; (- - -) FLT Model; (—) SSG Model; (\diamond) DNS results. (a) b_{11} , (b) b_{22} and (c) b_{12} .

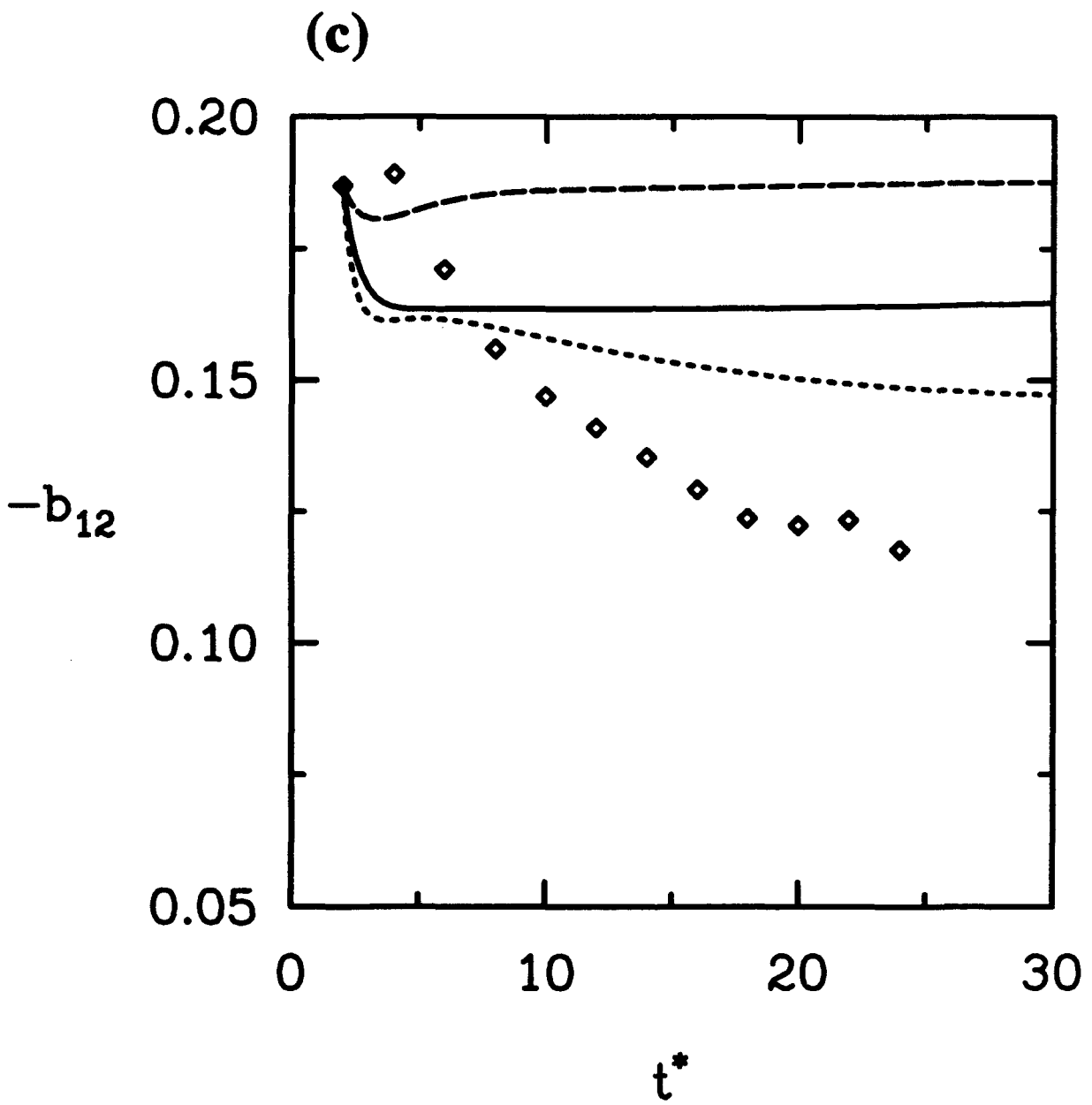


Figure 10. Time evolution of the Reynolds stress anisotropies: Comparison of the model predictions (with the dilatational terms of Sarkar *et al* [14, 15]) and the DNS results of Blaisdell *et al* [3] for compressible homogeneous shear flow. (—) LRR Model; (- - -) FLT Model; (—) SSG Model; (\diamond) DNS results. (a) b_{11} , (b) b_{22} and (c) b_{12} .

REPORT DOCUMENTATION PAGE			Form Approved OMB No. 0704-0188
<p>Public reporting burden for this collection of information is estimated to average 1 hour per response, including the time for reviewing instructions, searching existing data sources, gathering and maintaining the data needed, and completing and reviewing the collection of information. Send comments regarding this burden estimate or any other aspect of this collection of information, including suggestions for reducing this burden, to Washington Headquarters Services, Directorate for Information Operations and Reports, 1215 Jefferson Davis Highway, Suite 1204, Arlington, VA 22202-4302, and to the Office of Management and Budget, Paperwork Reduction Project (0704-0188), Washington, DC 20503.</p>			
1. AGENCY USE ONLY(Leave blank)	2. REPORT DATE	3. REPORT TYPE AND DATES COVERED	
	March 1994	Contractor Report	
4. TITLE AND SUBTITLE EVALUATION OF REYNOLDS STRESS TURBULENCE CLOSURES IN COMPRESSIBLE HOMOGENEOUS SHEAR FLOW		5. FUNDING NUMBERS C NAS1-19480 WU 505-90-52-01	
6. AUTHOR(S) C.G. Speziale R. Abid N.N. Mansour			
7. PERFORMING ORGANIZATION NAME(S) AND ADDRESS(ES) Institute for Computer Applications in Science and Engineering Mail Stop 132C, NASA Langley Research Center Hampton, VA 23681-0001		8. PERFORMING ORGANIZATION REPORT NUMBER ICASE Report No. 94-17	
9. SPONSORING/MONITORING AGENCY NAME(S) AND ADDRESS(ES) National Aeronautics and Space Administration Langley Research Center Hampton, VA 23681-0001		10. SPONSORING/MONITORING AGENCY REPORT NUMBER NASA CR-194892 ICASE Report No. 94-17	
11. SUPPLEMENTARY NOTES Langley Technical Monitor: Michael F. Card Final Report To appear in ZAMP			
12a. DISTRIBUTION/AVAILABILITY STATEMENT Unclassified-Unlimited Subject Category 34		12b. DISTRIBUTION CODE	
13. ABSTRACT (Maximum 200 words) Direct numerical simulation data bases for compressible homogeneous shear flow are used to evaluate the performance of recently proposed Reynolds stress closures for compressible turbulence. Three independent pressure-strain models are considered along with a variety of explicit compressible corrections that account for dilatational dissipation and pressure-dilatation effects. The ability of the models to predict both time evolving fields and equilibrium states is systematically tested. Consistent with earlier studies, it is found that the addition of simple dilatational models allows for the prediction of the reduced growth rate of turbulent kinetic energy in compressible homogeneous shear flow. However, a closer examination of the equilibrium structural parameters uncovers a major problem. None of the models are able to predict the dramatic increase in the normal Reynolds stress anisotropies or the significant decrease in the Reynolds shear stress anisotropy that arise from compressible effects. The physical origin of this deficiency is attributed to the neglect of compressible terms in the modeling of the deviatoric part of the pressure-strain correlation.			
14. SUBJECT TERMS Compressible turbulence, Homogeneous shear flow, Reynolds Stress Closures			15. NUMBER OF PAGES 30
			16. PRICE CODE A03
17. SECURITY CLASSIFICATION OF REPORT Unclassified	18. SECURITY CLASSIFICATION OF THIS PAGE Unclassified	19. SECURITY CLASSIFICATION OF ABSTRACT	20. LIMITATION OF ABSTRACT

NSN 7540-01-280-5500

★U.S. GOVERNMENT PRINTING OFFICE: 1994 - 528-064/86146

Standard Form 298 (Rev. 2-89)
Prescribed by ANSI Std. Z39-18
298-102